Nonlinear Controller of Single-Stage Photovoltaic Multicellular Inverter System

Taghzaoui Chaimaa, Abouloifa Abdelmajid, Elallali Aicha, Mchaouar youssef, Hamdoun Abdelatif
LTI Lab
HASSAN II University of Casablanca, Faculty of Science Ben M'sik
Casablanca, Morocco
taghzaouichaimaa@gmail.com, abouloifa@yahoo.fr,
aichaelallali@gmail.com, uns1mchaouar@gmail.com, alhamdoun@yahoo.fr

Lachkar Ibtissam
LISER Lab
HASSAN II University of Casablanca, ENSEM Casablanca
Casablanca, Morocco
lachkaribtissam@gmail.com

Abstract

In this paper, we are considering the problem of controlling a single-phase 3-celles inverter with LC output filter connected photovoltaic systems. The control objectives are: i) achievement of the maximum power point tracking (MPPT) for the PV array ii) ensuring a good convergence of the voltages across the flying capacitors iii) generating a perfectly sinusoidal voltage to the inverter output with amplitude and frequency fixed by the reference signal. The controller is designed using the backstepping approach in its adaptive versions and the Lyapunov stability argument. The whole system is described by 6^{th} order nonlinear mathematical model and controlled by using the backstepping approach and tools from Lyapunov stability. To demonstrate the performance of methods, some results of the overall system simulations are presented under MATLAB/Simulink software.

Keywords

Multicellular Converter**,** MPPT, Lyapunov stability, Backstepping approach.

1. INTODUCTION

In the last years, new energy sources have been proposed and have been developed due to the dependency and constant increase of costs of fossil fuels. On other hand, fossil fuels have a huge negative impact on the environment. In this context, local generation of heat and electricity and the local use of renewable energy resources are considered as some of the most promising options to provide a more secure, clean and more efficient energy supply. Among these renewable energy sources, photovoltaic (PV) technology has received a great attention because of distinctive advantages such as simplicity of allocation, high dependability, low maintenance, absence of fuel cost and lack of noise. In addition to these factors, there are other advantages such as the declining cost and prices of solar modules. Hence, the need to master series connection has grown because of the increased market of high-power applications and the significant decrease in semiconductors performance with the voltage rating. Thus, twenty years ago, Meynard and Foch (1992a), (1992b) have proposed the multicellular, also called converter flying capacitor multicellular (FCM), as a multilevel converter. Recently, this topology becomes one of the solutions used for the conversion of energy for strong powers in the industrial workplace. This kind of power converters is used in large scale PV applications for its superior advantages such as lower switching power dissipation, lower harmonic distortion and lower electromagnetic interference (EMI) outputs.
Several strategies for control have been proposed in the literature in order to improve the characterization of this converter for example: sliding modes in (Morvan et al., 2004; Amet et al., (2011, 2012); Djemaï et al., 2016), hybrid

control in (Elmetennani et al., 2016; Benmiloud et al., (2016a, 2016b)), predictive control in (Patino et al., (2008,2011); Defay et al., (2007, 2008)) and passivity based control in (Cormerais et al., 2008).
In general, the power converter interface from the DC source to the load or to the grid consists of two-stage converter: the DC/DC converter and the DC/AC converter. The DC-DC converter, which is used to buck, boost, buck-boosts the PV output voltage of PV panels as well as MPPT. In some paper, such as (Elmetennani et al., 2016), authors suggested the multicellular inverter instead of a classical DC–DC converter for boosting the output voltage with self MPPT capability to eliminate DC–DC converter, to take advantage of the properties of its particular topology, by sharing the constraints in voltage while working in high voltage installations. In the classical solution with two-stage converter, the DC/DC converter requires several additional devices producing a large amount of conduction losses, sluggish transient response and high cost while the advantages of the single stage converters are: good efficiency, a lower price and easier implementation. Despite the effectiveness of this approach, two-stage inverter systems tend to be exceedingly large and expensive. A single-stage topology could help to reduce the number of components, thereby reducing the physical size, increasing efficiency and facilitating implementation (Wu et al., 2011). An alternative solution could be the use of a single-stage converter where the DC/DC converter is avoided and in order to ensure the necessary DC/DC voltage level the PV array can be a string of PV panels or a multitude of parallel strings of PV panels.
In this paper, a new configuration of single phase, single-stage inverter system based on the FCM converter is proposed to increase the number of output voltage levels and as a result, reduce the output voltage THD with reduced ratings and losses of flying capacitors and semiconductors. We propose a nonlinear control of single-stage photovoltaic multicellular inverter system using backstepping approach and Lyapunov stability tools. The rest of the paper is organized as follows: the description and the modeling of the system are presented in section 2; section 3 is devoted to the controller design. Finally, the controller performances are illustrated through simulations under MATLAB/Simulink software in Section 4.

2. SYSTEM DESCRIPTION AND MODELING

2.1 Presentation of PV system

The proposed power system, presented in figure 1, is composed of a PV source with two DC link capacitors C_1 and C_2 on the DC side, a multicellular inverter and a low-pass output filter on the AC side in order to minimize the harmonics distortion of current and voltage. The structure of the serial multicellular inverter comprises 3 elementary switching cells in series, each switching cell of the converter is composed of pairs of complementary switches and controlled by a binary input signals μ_i and $\bar{\mu}_i$, where $\mu_i = 1$ ($\mu_i = 0$) indicates that the ith upper switch is closed (open) and the ith lower switch is open (closed). Between the two cells, a floating capacitor is inserted for high input voltage constraint share among the cells. The safe and proper functioning of the power converter directly depends on the suitable distribution of the voltages across each cell. That is why it is important to realise an internal regulation of the voltages across the terminals of the two capacitors.

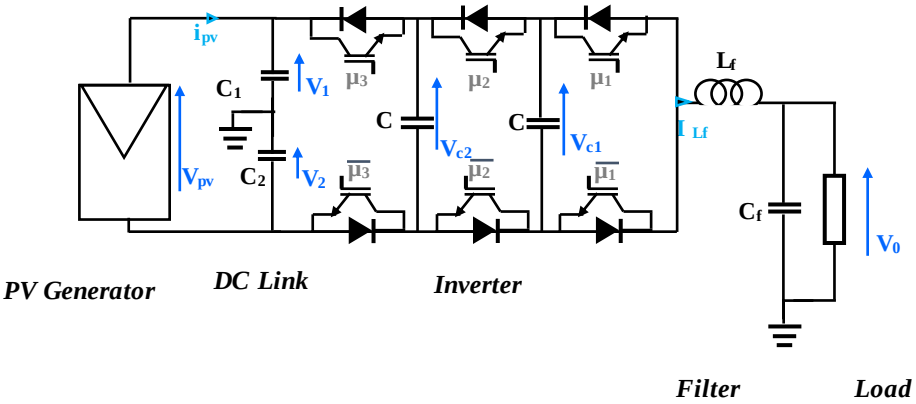

Figure 1. PV system with 3-cells inverter

2.2 PV array Model

Photovoltaic cells use the photovoltaic effect to convert sunlight irradiations energy to electric energy. Thus, the PV model used in this paper is based on the equivalent circuit (Bonkoungou et al., 2013) shown in Figure 2. This is the simplest equivalent circuit of a solar cell. The current source and diode represent the ideal behaviour of a solar cell, and the series and shunt resistors are used to model real-world losses such as current leaks and resistance between the metallic contacts and the semiconductor.

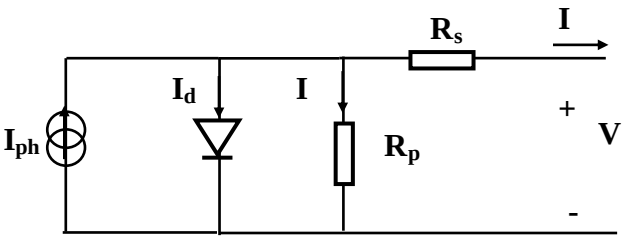

Figure 2. PV module equivalent circuit

where

- I_{ph} is the photocurrent (generated current under a given radiation).
- R_s is the series resistance.
- R_p is the shunt resistance.
- I denotes the PV array output current.
- V is the PV output voltage.

Using Kirchhoff's current law, the photovoltaic current equation can be represented by the equations (1a-d) as follows:

$$I = I_{ph} - I_d - I_r \tag{1a}$$

$$I = I_{ph} - I_0\left(exp\left(\frac{V + I\,R_s}{V_t}\right) - 1\right) - \left(\frac{V + I\,R_s}{R_p}\right) \tag{1b}$$

where $V_t = \dfrac{N\gamma KT}{q}$

$$I_0 = I_{0r}\left[\frac{T}{T_{ref}}\right]^3 exp\left[\frac{qE_{GO}}{\gamma K}\left(\frac{1}{T_{ref}} - \frac{1}{T}\right)\right] \tag{1c}$$

$$I_{ph} = I_{SC} + k_i\left(T - T_{ref}\right)\frac{\lambda}{100} \tag{1d}$$

where:

$\boldsymbol{T_r}$ is the reference temperature; $\boldsymbol{T}$ is the cell temperature;

$\boldsymbol{K}$ is the Boltzman's constant and $\boldsymbol{q}$ is the electron charge; $\boldsymbol{K_i}$ is the short circuit current temperature coefficient at $\boldsymbol{I_{sc}}$; $\boldsymbol{\lambda}$ is the solar radiation; $\boldsymbol{\gamma}$ is the ideality factor; $\boldsymbol{E_{GO}}$ is the band gap for silicon.

$\boldsymbol{I_o}$, $\boldsymbol{I_{or}}$ and $\boldsymbol{I_{sc}}$ represent respectively the cell reverse saturation current, the cell saturation current at $\boldsymbol{T_{ref}}$ and the short circuit current at 298,15K and 1 kW/m^2.

The photovoltaic generator (PVG) (also called PV array) is an assembly of many PV panels connected in N_s series and N_p parallel panels in order to provide the desired values of output voltage and current required for particular applications. The output voltage and current of a PVG can be given by the following equations:

$$V_m = N_s V \tag{1e}$$

$$I_m = N_p I \tag{1f}$$

The PV array module considered in this paper is composed by a solar panel array of 22 solar panels. The corresponding electrical characteristics are listed in Table 1.

Table 1. Electrical specifications for the solar module

Parameter	Symbol	Value
Maximum Power	P_m	200 W
Short circuit current	I_{sc}	8.21 A
Open circuit voltage	V_{oc}	32.9V
Maximum power voltage	V_m	26.3 V
Maximum power current	I_m	7.61A
Number of series cells	N_{sc}	54

2.3 PV system modeling

Applying Kirchhoff's laws, the general model of the PV chain with 3 cells converter under study is given by the following set of differential equations:

$$C_f \dot{v}_0 = i_{Lf} - \frac{v_0}{R} \quad (2a)$$

$$L_f \dot{i}_{Lf} = (\mu_1 - \mu_2) v_{c1} + (\mu_2 - \mu_3) v_{c2} + \mu_3 v_1 - v_0 \quad (2b)$$

$$C \dot{v}_{c1} = (\mu_2 - \mu_1) i_{Lf} \quad (2c)$$

$$C \dot{v}_{c2} = (\mu_3 - \mu_2) i_{Lf} \quad (2d)$$

$$C_1 \dot{v}_1 = i_{pv} - \mu_1 i_{Lf} \quad (2e)$$

$$C_2 \dot{v}_2 = i_{pv} - (1 - \mu_1) i_{Lf} \quad (2f)$$

$$\mu_i \in \{0,1\}, i = 1,2,3$$

where i_{Lf} , i_{pv} v_0 , v_1 , v_2 and $v_{ci}(i = 1,2)$ represent respectively measured values of the conductor current, the current generated by PV array, the output voltage, the voltage across the Dc link capacitor capacitors $C_i(i = 1,2)$ and Flying capacitor C . R , C_f and L_f represent respectively the resistive load, the filter capacitor, and the filter inductance.

For control design purpose, it is more convenient to consider the following averaged model obtained by averaging the model (2a-d) over one switching period.

$$C_f \dot{x}_1 = i_{Lf} - \frac{x_1}{R} \quad (3a)$$

$$L_f \dot{x}_2 = (u_1 - u_2) x_3 + (u_2 - u_3) x_4 + u_3 x_5 - x_1 \quad (3b)$$

$$C \dot{x}_3 = (u_2 - u_1) x_2 \quad (3c)$$

$$C \dot{x}_4 = (u_3 - u_2) x_2 \quad (3d)$$

Where x_1 , x_2 , x_3 , x_4 , x_5 and u_i denote the average values, over cutting periods, of the signals v_0 , i_{Lf} , v_{c1} , v_{c2} , v_1 and $\mu_i \in [0,1], i = 1,2,3$.

Note that the mathematical model (3a-d) is nonlinear because of the products involving the state variables and input signals. Taking into account these nonlinearities, a nonlinear controller using the backstepping approach will be done in the next paragraph.

3. CONTROLLER DESIGN

3.1 Control objectives

In order to define the control strategy, first one has to establish the control objectives, which must be formulated as following:

i. A perfect MPPT. Specifically, the controller must enforce the voltage the average value of the voltage V_{pv} provided by the solar array to track as possible a given desired value of the reference voltage V_{pv}^{*}. To achieve this objective, we use the well-known "Perturb and Observe algorithm" to generate the reference voltage signal.

ii. Regulate the capacitors voltages at its desired reference value.

$$x_3^* = \frac{V_{pv}^*}{3} \tag{4}$$

$$x_4^* = \frac{2V_{pv}^*}{3} \tag{5}$$

iii. generate a sinusoidal voltage in the network with amplitude and frequency fixed by the reference signal:

$$x_1^* = V\sqrt{2}sin(\omega t) \tag{6}$$

3.2 MPPT Control Algorithm

To ensure the correct operation of PV module at its maximum power point as the temperature, insolation and load vary, we use well known "perturb and observe algorithm (P&O). This algorithm uses simple feedback arrangement and little measured parameters. It is based on the following criterion: if the operating voltage of the PV array is perturbed in a given direction and if the power drawn from the PV array increases, this means that the operating point has moved toward the MPP and, therefore, the operating voltage must be further perturbed in the same direction. Otherwise, if the power drawn from the PV array decreases, the operating point has moved away from the MPP therefore, the direction of the operating voltage perturbation must be reversed and, when the stable condition is arrived the algorithm oscillates around the peak power point. (Jain and Agarwal, 2004; Atallah et al., 2014) The algorithm steps are described as shown in the following flowchart (figure 3) (Bhandari et al., 2014).The algorithm first calculates the power (P) by sensing the voltage and current. Then it provides a perturbation in the voltage based on the change of power, where the delta V_{pv} is known as the perturbed voltage, If delta V_{pv} is large, the convergence is fast but that causes large fluctuation in the steady state power and vice versa. The oscillation causes undesirable losses of PV power during steady state.

In order to maintain the power variation small the perturbation size is remain very small. The technique is advanced in such a Style that it sets a reference voltage of the module corresponding to the peak voltage of the module.

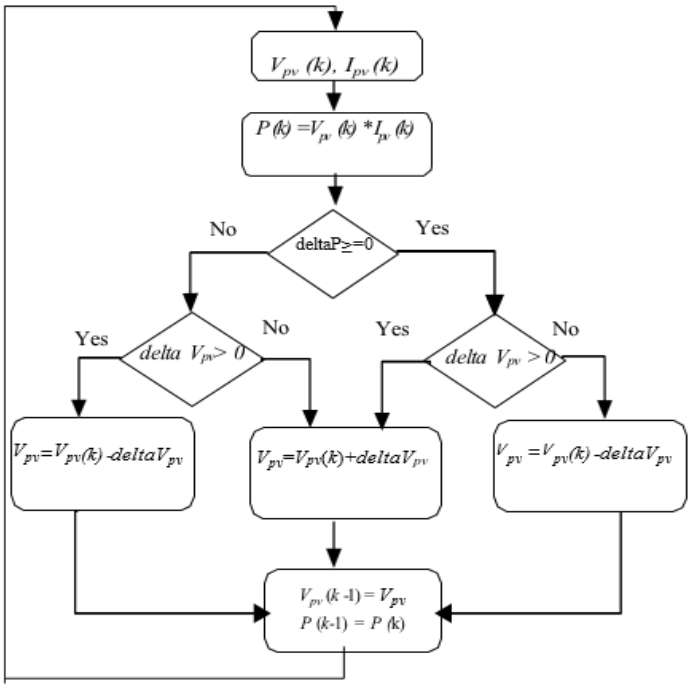

Figure 3. P&O flowchart.

3.3 Nonlinear controller design

Backstepping is a recently developed design tool for constructing globally stabilizing control laws for a certain class of nonlinear dynamic systems.it is a recursive procedure, which breaks a design problem for the full system into sequence of design problems for lower order systems. Backstepping designs by breaking down complex nonlinear systems into smaller subsystems. Then designing control Lyapunov functions and virtual controls for these systems and finally integrating these individual controllers into an actual controller, by stepping back through the subsystem and reassembling it from its component subsystems. (Arun Kumar et al., 2015)
Following the backstepping technique, the controller is designed in two steps.

- **Step 1**:

Let us define the following tracking error:

$$z_1 = C\left(x_3 - x_3^*\right) \tag{7a}$$

$$z_2 = C\left(x_4 - x_4^*\right) \tag{7b}$$

$$z_3 = C_f\left(x_1 - x_1^*\right) \tag{7c}$$

with x_3, x_4 and x_1 are respectively the measured capacitor voltage and the measured output voltage x_3^*, x_4^* and x_1^* represent respectively the desired trajectories of x_3, x_4 and x_1.

Deriving z_1, z_2 and z_3 with respect to time yields and accounting for (3a) and (3c-d), implies:

$$\dot{z}_1 = \left(u_2 - u_1\right)x_2 - C\,\dot{x}_3^* \tag{8a}$$

$$\dot{z}_2 = \left(u_3 - u_2\right)x_2 - C\,\dot{x}_4^* \tag{8b}$$

$$\dot{z}_3 = \left(x_2 - \frac{x_1}{R}\right) - C_f\,\dot{x}_1^* \tag{8c}$$

We need to select a Lyapunov function for such system. As the objective is to drive its state $\left(z_1, z_2, z_3\right)$ to zero, it is natural to choose the following function:

$$V_1 = 0.5\,z_1^2 + 0.5\,z_2^2 + 0.5 z_3^2 \tag{9a}$$

Its time derivative is given by the following equation:

$$\dot{V}_1 = z_1\,\dot{z}_1 + z_2\,\dot{z}_2 + z_3\,\dot{z}_3 \tag{9b}$$

The choice $\dot{V}_2 = -\lambda_1 z_1^2 - \lambda_2 z_2^2 - \lambda_3 z_3^2$, where $\lambda_i\left(i = 1,...,3\right)$ are positive constants of synthesis, leads to a Lyapunov candidate function whose dynamics is negative definite. In view of (9b) and using (8a-c) this suggests the following choices:

$$\left(u_2 - u_1\right)x_2 - C\,\dot{x}_3^* = -\lambda_1 z_1 \tag{10a}$$

$$\left(u_3 - u_2\right)x_2 - C\,\dot{x}_4{}^* = -\lambda_2 z_2 \tag{10b}$$

$$\left(x_2 - \frac{x_1}{R}\right) - C_f\,\dot{x}_1^* = -\lambda_3 z_3 \tag{10c}$$

if we choose x_2 as virtual control input, we deduce the stabilizing function namely x_2^*:

$$x_2^* = -\lambda_3\,z_3 + \frac{x_1}{R} + C_f\,\dot{x}_1^* \tag{11}$$

As x_2 is not the control input, a new error variable z_4 between the virtual control x_2 and its desired value x_2^* is introduced:

$$z_4 = L_f\left(x_2 - x_2^*\right) \tag{12}$$

Then, using (11) and (8c), dynamics of error z_3 became:

$$\dot{z}_3 = \frac{z_4}{L_f} - \lambda_3\,z_3 \tag{13}$$

In the same way

$$\dot{V}_1 = -\lambda_1 z_1^2 - \lambda_2 z_2^2 - \lambda_3 z_3^2 + \frac{z_3\, z_4}{L_f} \tag{14}$$

- **Step 2**:

The objective now is to enforce the error variables (z_1, z_2, z_3, z_4) to vanish. To this end, let us first determine the dynamics of z_4 , we obtain:

$$\dot{z}_4 = (u_1 - u_2)x_3 + (u_2 - u_3)x_4 + u_3 x_5 - x_1 - L_f \dot{x}_2^* \tag{15}$$

We are finally in a position to make a convenient choice of the parameter update law and feedback control to stabilize the whole system with state vector (z_1, z_2, z_3, z_4) Consider the augmented Lyapunov function candidate.

$$V_2 = V_1 + 0.5 z_4^2 \tag{16a}$$

Its dynamics is given by:

$$\dot{V}_2 = \dot{V}_1 + z_4 \dot{z}_4 \tag{16b}$$

$$\dot{V}_2 = -\lambda_1 z_1^2 - \lambda_2 z_2^2 - \lambda_3 z_3^2 + z_4\left(\frac{z_3}{L_f} + \dot{z}_4\right) \tag{16c}$$

As our goal is to make $\dot{V}_2$ non-positive definite $\dot{V}_2 = -\lambda_1 z_1^2 - \lambda_2 z_2^2 - \lambda_3 z_3^2 - \lambda_4 z_4^2 \le 0$, this suggests choosing that the bracketed term, on the right side of (16c), is equal to $-\lambda_4 z_4$:

$$\dot{z}_4 = -\lambda_4\, z_4 - \frac{z_3}{L_f} \tag{17}$$

The equations (15) and (17) lead to:

$$-\lambda_4\, z_4 - \frac{z_3}{L_f} = (u_1 - u_2)x_3 + (u_2 - u_3)x_4 + u_3 x_5 - x_1 - L_f \dot{x}_2^* \tag{18}$$

where λ_4 is a positive constant of synthesis.

Finally, the control input can be solved from the following systemequations.

$$u_3 = \frac{(u_2 - u_1)x_3 + (u_3 - u_2)x_4 + L_f\, \dot{x}_2^* + x_1 - \dfrac{C_f\,(x_1 - x_1^*)}{L_f} - \lambda_4\, L_f\,(x_2 - x_2^*)}{x_5} \tag{19}$$

$$u_2 = u_3 - \frac{C\,\dot{x}_4^* - \lambda_2\, C\,(x_4 - x_4^*)}{x_2} \tag{20}$$

$$u_1 = u_2 - \frac{C\,\dot{x}_3^* - \lambda_1\, C\,(x_3 - x_3^*)}{x_2} \tag{21}$$

4. SIMULATION RESULTS

The proposed control system will have the structure shown in Figure 4. The controller will be synthesized by a technique using Backstepping approach, and validated through simulations performed using the Matlab/Simulink and its SimPower SystemToolbox.

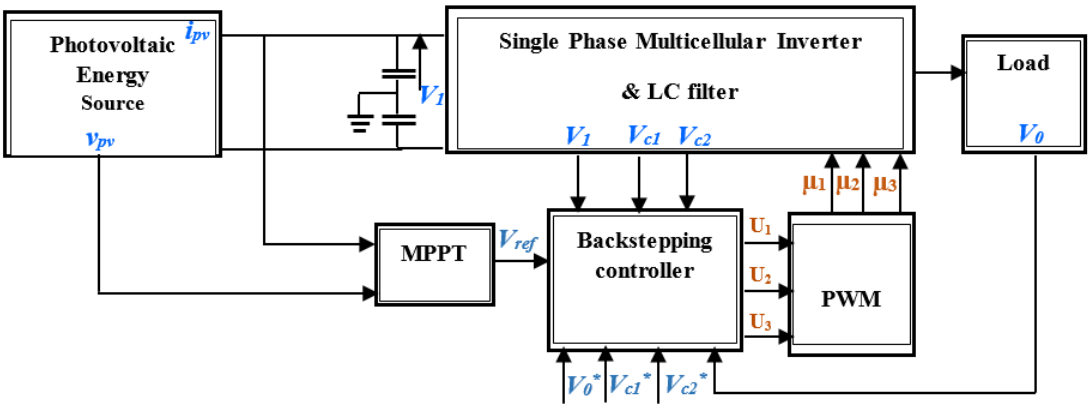

Figure 4. Control block for multicellular inverter

The characteristics of the controlled system are listed in table 2. Backstepping controller parameters, which proved to be convenient, are given values of table 3, and the simulation results have been obtained under standard climatic conditions (1000 W/m² and 25°C).and the resulting control performances are shown by Figures 5 to 8.

Table 2. Main parameters values of simulated circuit

Components	symbol	Value
Flying capacitor	C	4000 µF
Dc link capacitors	C_2,C_1	3 mF
Filter capacitor	C_f	9 µF
Filter inductor	L_f	1 mH
Load impedance	R	35 Ω

Table 3. Backstepping controller parameters

Parameter	Value
λ_1	180
λ_2	400
λ_3	8000
λ_4	2000

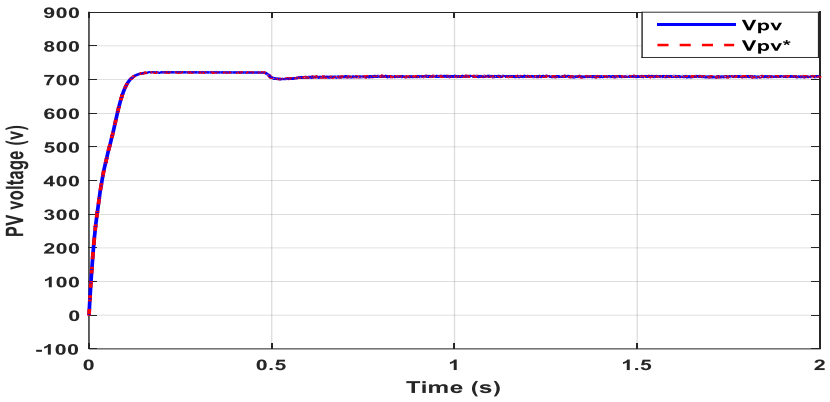

Figure 5. PV voltage with its reference

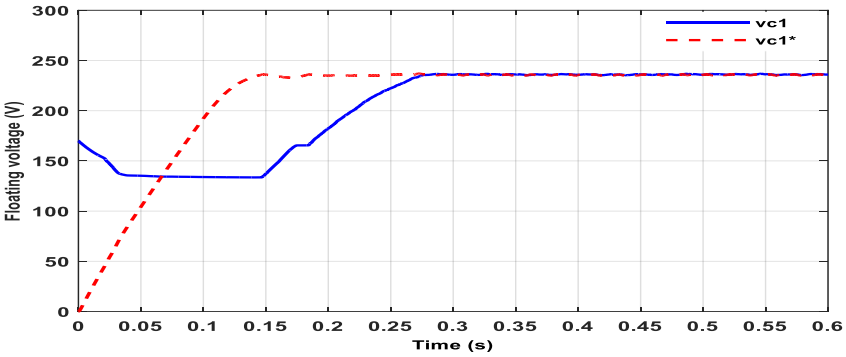

Figure 6. Actual and desired voltage of cell-1's flying capacitor (v_{C1})

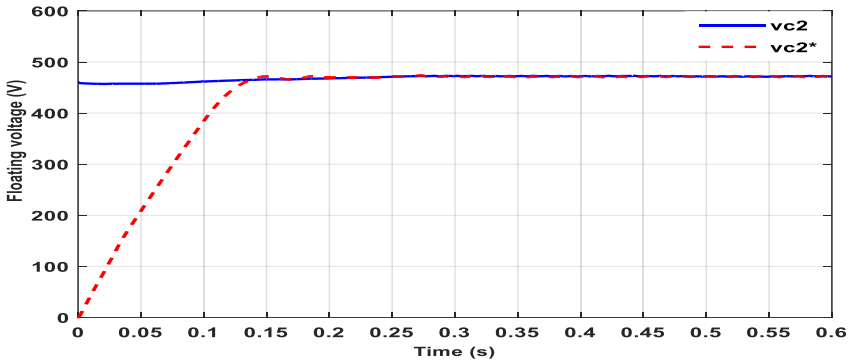

Figure 7. Actual and desired voltage of cell-2's flying capacitor (v_{c2})

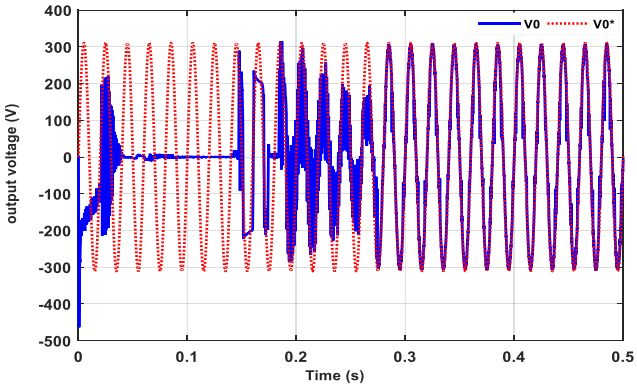

Figure 8(a). Actual and desired output voltage v_0

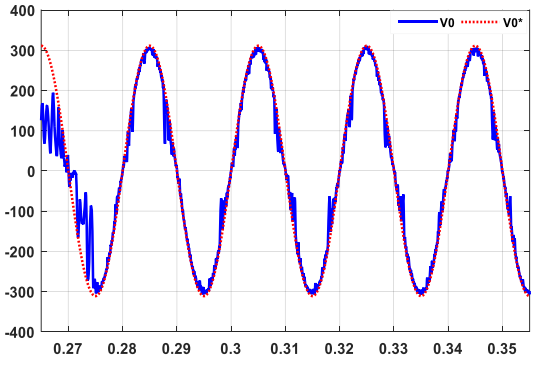

Figure 8(b). Zoom of output voltage v_0

Figure 5 shows the evolution of the converter input voltage, in particular it is noted that this voltage follows the reference voltage generated by the "P&O" algorithm. The capacitor voltages v_{c1} and v_{c2} shown in Figures (6-7) converge towards their desired values given by (4) and (5), after 0.27 seconds they reach their references voltages. Figure 8 shows that the output voltage v_0 is sinusoidal reaches the desired voltage $220\sqrt{2}sin(100\pi t)$ at time 0.275 seconds.

5. Conclusion

The present paper is focusing on the problem of controlling single stage multicellular inverter. The latter is described by sixth order nonlinear averaged model. The synthesis of the regulator was achieved by having recourse to advanced tools of nonlinear control such as stability in the sense of Lyapunov. It is formally shown by simulation under Matlab/Simulink that the proposed controller guarantees the desired tracking performance and satisfies all the objectives for which it was designed, namely: i) maximum power point tracking (MPPT) of (PV) module; ii) Regulating the voltages of the capacitors to their desired reference levels and iii) generating a sinusoidal voltage at the output.

References

Ahmed, M. Atallah, Almoataz Y. Abdelaziz, and Raihan S. Jumaah., Implementation of perturb and observe MPPT of PV system with direct control method using buck and buck-boost converters, *Emerging Trends in Electrical, Electronics & Instrumentation Engineering: An international Journal (EEIEJ),* Vol. 1, no. 1, pp. 31-44, 2014.

Amet, L. Ghanes, M. and Barbot, J. P., Commande directe d'un convertisseur multicellulaire: résultats expérimentaux, *CIFA – 7ème Conférence Internationale Francophone d'Automatique*, 2012.

Amet, L., Ghanes, M., and Barbot, J., Direct control based on sliding mode techniques for multicell serial chopper, *American Control Conference (ACC),* pp. 751– 756, 2012.

Arun Kumar, V V., and Laila Beebi, M., Adaptive Backstepping Sliding Mode Control for Roll Channel of Launch Vehicle, *Int J Aeronautics Aerospace Res*. Vol.2, no. 5, pp. 58-64, 2015.

Benmiloud, M., and Benalia, A., Finite-time stabilization of the limit cycle of two-cell DC/DC converter: hybrid approach, *Nonlinear Dyn*, vol. 83, pp. 319–332, 2016.

Benmiloud, M., Benalia, Defoort, M., and Djemaï M., On the limit cycle stabilization of a DC/DC three-cell converter, *Control Engineering Practice*, Vol. 49, pp. 29-41, April 2016.

Bhandari, B., Poudel, S., Kyung-Tae, L., and Sung-Hoon, A., Mathematical Modeling of Hybrid Renewable Energy System: A Review on Small Hydro-Solar-Wind Power Generation, *International Journal of Precision Engineering and Manufacturing Green Technology*, Vol.1, no. 2, pp. 157-173, 2014.

Bonkoungou, D., Koalaga, Z., and Njomo, D., Modelling and Simulation of Photovoltaic Module Considering Single-Diode Equivalent Circuit Model in MATLAB, *International Journal of Emerging Technology and Advanced Engineering* vol.3, no. 3, pp. 493–502, 2013.

Defay, F. Llor, A., and Fadel, M., An active power filter using a sensorless muticell inverter, *in Proc. IEEE ISIE*, pp. 679–684. 2007.

Defaÿ, F. Llor, A.M., and Fadel, M., A., Predictive Control with Flying Capacitor Balancing of a Multicell Active Power Filter, *IEEE TRANSACTIONS ON INDUSTRIAL ELECTRONICS*, Vol. 55, No 9, pp. 3212-3220, 2008.

Djemaï, M., Busawon, K., Benmansour, K., and Marouf, A., High-Order Sliding Mode Control of a DC Motor Drive Via a Switched Controlled Multi-Cellular Converter, *International Journal of Systems Science*, Vol. 42, pp. 1869-1882, 2011.

Hosseini, S.H., Khoshkbar Sadigh, A., and Sharifi, A., Estimation of flying capacitors voltages in multicell converters, *6th Int. Conf. on Electrical Engineering/Electronics Computer Telecommunications and Information Technology*, pp. 110-113, 2009.

Jain, S., and Agarwal, V., A new algorithm for rapid tracking of approximate maximum power point in photovoltaic systems, *IEEE Power Electron.Lett*., vol. 2, no. 1, pp. 16–19, Mar. 2004.

Meynard, T., and Foch, H., French patent N91. 09582 du 25 juillet 1991; dpt. international PCT (Europe, Japon, USA, Canada) N92. 00652 du 8 juillet 1992, 1992.

Meynard, T., and Foch, H., Multilevel choppers for high voltage applications, *EPEJ 2 (March (1)) 1992*, 1992

Meynard, T.A., Fadel, M., and Aouda, N., Modeling of multilevel converter, *IEEE Trans. Ind. Electron*., Vol. 44, no.3, pp. 356-364, 1997.

Morvan, C., Richard, P.Y, Cormerais, H., and Buisson, J., Sliding mode control of switching systems with Boolean inputs, in: *IFAC Conference NOLCOS, Stuttgart Allemagne*, pp.747-752, September 2004.

Turpin, C., Deprez, L., Forest, F., Richardeau, F., and. Meynard, T.A., A ZVS imbricated cell multilevel inverter with auxiliary resonant commutated poles, *IEEE Trans. Power Electron*., Vol.17, no. 6, pp. 874-882, 2002.

Wu, Chang, C.H., Lin, L.C., and Kuo, C.L., Power Loss Comparison of Single- and Two-Stage Grid Connected Photovoltaic Systems, *IEEE Transactions on Energy Conversation*, Vol. 26, pp. 707-715, 2011.

Biography

Taghzaoui Chaimaa is a doctoral student in LTI laboratory, Hassan II of Casablanca University. He holds a Master's degree in information processing (2015) and a bachelor's degree in Electronics and Industrial data processing (2013).Her research interests focus on the area of simulation, modeling, Nonlinear Control and observation of converters.

Elallali Aicha: She holds a Bachelor degree in Electronic and Industrial data processing (2013) and a Master in Information Processing (TI) (2015) from Hassan II University of Casablanca. Currently in the second year of a Doctorate at the Hassan II University of Casablanca, in LTI laboratory, under the direction of Pr. Hamdoun Abdelatif on a thesis entitled "Multi-level inverters used in active filtering". In addition to the participation in an international symposium and an international communication on the monitoring of industrial systems, 19-20 October 2016, Fez, Morocco, and the 8th National Meeting of Young Researchers in Physics, Department of Physics Faculty of Science Ben M'Sik, there is a work submitted to an international conference in Toulouse, as well as the preparation of an article to be submitted to an indexed journal.